Molecular and cellular characterization of cardiac overload-induced hypertrophy and failure

Umar, S.

Citation

Umar, S. (2009, June 18). *Molecular and cellular characterization of cardiac overload-induced hypertrophy and failure*. Retrieved from https://hdl.handle.net/1887/13860

Chapter 8

An exploration of the role of Kv channels in excitability of right ventricular cardiomyocytes from normal adult rats

S. Umar
W. P. M. van Meerwijk
D. A. Pijnappels
M. J. Schalij
A. van der Laarse
D. L. Ypey

Abstract

Purpose: In the present study we analyzed mechanisms of excitability of right ventricular myocytes (RVMCs) isolated from the adult rat heart, making use of the naturally occurring variability of excitability of these cells. We focused on the role of voltage-activated K$^+$ currents (*Ikv*) in shaping the current pulse-evoked action potential (AP) and in generating sustained depolarizing current-induced automaticity (DIA).

Methods: Membrane potentials and currents were measured with the whole-cell patch-clamp technique in current- and voltage-clamp configuration, respectively, with standard-normal intra- and extracellular solutions. Simulation experiments were carried out with a computer model describing the electrophysiology of the RVMC of the rat (Pandit *et al.*, 2001, 2003).

Results: The resting conditions were characterized by a resting membrane potential (RMP) of ~-70 mV, a membrane resistance at RMP of ~111 MΩ, and a membrane capacitance (Cm) of ~173 pF (17-20 cells). Voltage-clamp experiments revealed the variable expression of voltage-activated Na$^+$ current (*Inav*), inward rectifier K$^+$ current (*Ikir*) and voltage-activated K$^+$ current (*Ikv*), including the transient current *It* and sustained current *Iss* (20 cells). L-type calcium current (*IcaL*) was recognized during inactivation of *Inav* and *Ikv* by a holding potential of –40 mV. APs evoked by current-clamp pulses were variable in amplitude and duration, probably due to the variable (endo-, meso- and epicardial) origin of the myocytes. AP-properties are described for two example groups: (**1**) High-peak/Long-duration APs (HL-APs) with AP-peak amplitudes of 30-40 mV and AP-durations of 50-110 ms at half AP-height, and (**2**) Low-peak/Short-duration APs (LS-APs) with peaks of -10 to +10 mV and durations of 20-30 ms. AP-amplitude and duration in the whole population were negatively correlated with *It* expression, indicating that activation of *It* upon activation of *Inav* lowers the degree of activation of *IcaL* during AP-generation. DIA was usually recorded as an after-effect of the first AP upon applying the sustained current, but it was always transient with 1-6 afterwaves within the first 1.6 s. DIA was critically dependent on the strength of the sustained current and occurred at membrane potentials >-40 mV, where all *Ina* and most *Ikv* are becoming inactivated. DIA was inhibited by 10 μmol/L nifedipine (n=4) but was not clearly dependent on the size of *It*. This indicates that the automaticity mechanism of DIA largely depends on the properties of *IcaL* as an inward current. Model experiments reproduced the decrease of AP-duration with an increase in *It* and revealed a DIA-mechanism based on *IcaL* deinactivation and *Iss* deactivation at depolarized potentials.

Conclusion: We discuss these results in terms of their implications for understanding normal RVMC excitability and for arrhythmogenic mechanisms in heart failure.

Introduction

While investigating in a recent study the effect of stem cell therapy on heart failure related changes in the electrophysiology of right ventricular myocytes (RVMCs) from hearts of rats with experimental pulmonary arterial hypertension, we were confronted with a much greater variability in excitability in these RVMCs, normal or diseased, than anticipated from the literature (Lee *et al.*, 1997 and Pandit *et al.*, 2001 & 2003). For example, one group of cells had a strongly reduced excitability as apparent from very low peak-height (at membrane potential Vm<0 mV) and short-duration (~25 ms) action potentials (APs), while another group had normal peak-height (at Vm~+40 mV) and very long-duration (~100 ms) APs. This hampered comparison of the excitability properties of RVMCs from normal, diseased and stem cell-treated animals and required a preliminary electrophysiological study of RVMCs from normal rats to characterize and explain this variability.

One of the reasons why RVMCs are heterogeneous in their excitability properties is that they have a mixed histological endo-, meso- and epicardial origin (Clark *et al.*, 1993; Antzelevitch *et al.*, 2000). From a mechanistic point of view, variability may be a great source of information for understanding the functional consequences of electrophysiological differences between heart cells. This is of particular importance, as insights in mechanisms of normal and abnormal AP-shaping and of regular and irregular heart rhythm generation are still limited, despite intensive experimental and theoretical research on this subject (Pandit *et al.*, 2001, 2003; Pogwizd and Bers, 2004; Antoons *et al.*, 2007). Therefore, we have analyzed the variability in excitability of normal adult rat RVMCs by systematically comparing the current-clamp properties of the cells (excitability) with the voltage-clamp properties (ion channel expression) of the same cells under standard-normal conditions. Besides studying AP-shaping by the various ion channel types, we also studied the ionic mechanism of generating depolarizing current-induced automaticity (DIA), a mode of excitability of ventricular myocytes that has been studied before as a model for arrhythmogenesis 'from abnormal automaticity' mainly in other species of mammals than the rat (Katzung, 1975; Malecot *et al.*, 1985; Peters *et al.*, 2000). By contrasting the DIA-mode excitability under sustained current stimulation with that of current-pulse evoked APs in patch-clamp experiments and by theoretical modeling, we aimed to answer questions about the particular role of Kv-currents (*Ikv*) in pulse-evoked AP-shaping and in generating DIA.

Because we were primarily interested in the role of the electrical membrane properties in cardiomyocyte excitability, we excluded intracellular calcium dynamics by using the calcium buffer EGTA. This also prevented a significant role of the sodium/calcium-exchanger (NCX) in the measured myocyte excitability (cf. Pogwizd and Bers, 2004).

The model of Pandit *et al.* (2001, 2003) was used to explore mechanistic explanations of the observed excitability properties of rat RVMCs. A particular result was that the model simulations revealed that DIAs occurred as a result of the kinetic properties of *IcaL* and *Iss*.

The present results provide a basis for analyzing differences in excitability between ventricular myocytes from normal rats and from rats with experimental heart failure. They may also provide clues for a better understanding of mechanisms of heart failure- related ventricular arrhythmias.

Materials and Methods

Animals and ventricular myocyte isolation

Rats were treated in accordance with the national guidelines and with permission of the Animal Experiments Committee of the Leiden University Medical Center. The animals were housed, two animals per cage, with a 12:12-h light-dark cycle and an unrestricted food and water supply. Three-month old female Wistar rats weighing 200-250 g (Harlan, Zeist, the Netherlands) were used.

Cardiomyocyte isolation

The rat was anaesthetised, and the thorax was opened. The heart was taken out quickly and immediately transferred to ice-cold, oxygenated Tyrode solution. The heart was mounted to a Langendorff perfusion set-up and then perfused for 5 min with an oxygenated Tyrode solution at constant pressure (70 mmHg) at 37° C. The perfusion fluid was replaced by an oxygenated, low calcium (10 μmol/L) perfusion fluid. Contractions disappeared within 30 s. After 5 min of low calcium perfusion, the perfusion was continued in a recirculating manner at a perfusion pressure of 60 mm Hg. At that time collagenase (0.06%) was added. Thirty min later, the flow rate was too high too maintain a perfusion pressure of 60 mm Hg. Then, the heart was removed and the right ventricle (RV) was separated from the left ventricle and the interventricular septum. RV was cut in small pieces, incubated in a fresh collagenase (0.06%) solution, and dissociated in a waterbath shaker at 37° C. After sedimentation of the myocytes, sedimented myocytes were resuspended and stored at 37° C in fresh HEPES-buffered salt solution containing (in mmol/L) NaCl 125, KCl 5, $MgSO_4$ 1, KH_2PO_4 1, $CaCl_2$ 1.8, $NaHCO_3$ 10, HEPES 20, glucose 5.5, pH 7.4. The average fraction of rod-shaped myocytes was 80 %. The percentage of rod-shaped myocytes decreased by about 10 % during 6 h at 37° C.

Whole-cell patch-clamp experiments

Membrane potentials (Vm) and membrane currents (*Im*) of right ventricular myocytes (RVMCs) from 22 cells from 5 rats were measured with the patch-clamp technique in the whole-cell current-clamp and voltage-clamp configuration, respectively. The recordings were performed at 21°C with an L/M-PC amplifier (List-Medical, Darmstadt, Germany), set at 3 KHz filtering. pClamp/Clampex8 software (Axon Instruments, Molecular Devices, Sunnyvale, CA, USA) was used for data acquisition and off-line analysis. The bath solution contained (in mmol/L) NaCl 137, KCl 5, $MgCl_2$ 1, $CaCl_2$ 1.8, HEPES 10, and glucose 11, pH 7.4, while the pipette solution contained (in mmol/L) Na_2ATP 6, KCl 115, $MgCl_2$ 1, EGTA 5 and HEPES 10, pH 7.4). Pipette resistance (Rpip) was 2.8$\pm$0.4 MΩ (n=20), seal

resistance (Rseal) was 4.1 ± 1.3 GΩ (n=13), and series resistance (Rser) was 6.6 ± 3.1 MΩ (n=20). Pipette potential offsets (Vpips) developing during the experiments were usually between +1 and –2.3 mV, and were not corrected for. Larger offsets were corrected in 3 cells.

In order to be able to check Rser and Cm-measurements, Rser was not compensated and the slow capacitive transients were not cancelled. Rser-values apply to the immediately preceding or following voltage-clamp tests, because Rser tended to increase during the experiment. Whole-cell recordings after gigasealing (n=20) were accepted for analysis if the membrane potential stabilized within a few minutes and if the membrane resistance measured in voltage-clamp at –60 mV (Rm(-60)) was >100 MΩ (to avoid leaky membranes). Voltage-drop artifacts across Rser during current-clamp stimulation (usually <10 mV) were corrected for, except when they were <2 mV. Voltage errors across Rser during voltage-clamp were usually <30 mV (<5nA times 6MΩ).

This was only considered acceptable for large driving forces, such as during *Ikv* recording at +60 mV, where the ideal driving force (Vm-Ek)=144 mV and the real driving force is <20% smaller because of the <30-mV drop in voltage across Rser. This kind of measurement error was confirmed in our model simulations (see below). We, therefore, realize that our Rser-values are too large to reliably measure maximal values of *Inav, Ikir* and *Ikv*. So, the average values of these currents presented in Table 1, measured at potentials where contamination with other currents is small, should still be considered as underestimates. Nevertheless, the Rser values were good enough to allow identification of these currents and to detect the activation potentials of these currents for current detection levels within 0.5 nA (<2% voltage error). For a rough quantitative measurement of *Ikv*, its peak, *Ikvp*, was measured at +60 mV, not only because its driving force is large at that potential, but also because *Inav* and *IcaL* are minimal at that potential, since their reversal potentials are close to +60 mV (see Figs. 3 and 5). The amplitude of *It* was determined by subtracting the sustained *Ikv* (*Iss*) at 60 mV, approximated by the current at t=180 ms, from the peak *Ikv* (*Ikvp*). This procedure also included subtraction of leak current in the calculation of *Itp*. To minimize disturbing effects of variability in *Itp*-values related to a variability in cell size, *Itp* values were corrected for cell size by dividing *Itp* by Cm.

Modeling

We have used the computer model of the rat ventricular myocyte made by Pandit *et al.* (2001, 2003) to explore both the excitability mechanism of current-pulse evoked action potentials (pAPs) and that of depolarizing-current induced automaticity (DIA) in the RVMC of the adult rat.

The model of Pandit *et al.* (2001, 2003) is a Hodgkin-Huxley type membrane model coupled to an intracellular ion-dynamics model via the intracellular concentrations of Ca, Na and K. It can be used in a left-epicardial and left-endocardial myocyte version (Pandit *et al.*, 2001) and in a right-epicardial one (Pandit *et al.*, 2003).

The membrane model is largely based on published experimental work and contains the currents identified in the present experiments (Ikir, Inav, Ikv (It and Iss), IcaL) together with two other currents of smaller amplitude (If and background current Ib) and with the electrogenic currents of the ion transporters the sodium-calcium exchanger (NCX), the Na^+, K^+-ATPase and the plasma membrane calcium ATP-ase (PMCA). Dr. Pandit has kindly provided us with a list of misprint-corrections (including 5 obvious sign errors in exponentials) to allow us to make proper runs with the model (personal communication, 2008).

We have extended the model with the electrical connection of the pipette to the cell in order to be able to account for the non-ideal voltage- and current-clamp properties of the measurements (large series resistance Rser). We have used the model as a plasma membrane model uncoupled from intracellular calcium signaling and ion changes by setting the intracellular concentrations of $[Ca^{2+}]_i$=79 nmol/L, $[Na]_i$=10.7 mmol/L, and $[K]_i$=139.3 mmol/L, which conditions approximate the conditions in our ruptured whole-cell experiments with EGTA in the pipette.

Statistics

Groups of observations are described as means $\pm$ SD (n), unless mentioned otherwise. Correlation analysis is performed with nonparametric (Spearman) tests. We used the SPSS software (SPSS Inc., Chicago, IL, USA). A *p*-value <0.05 is considered to represent a significant test result.

Results

Basic electrical properties of adult rat RVMCs

Basic electrical membrane properties such as the RMP, Rm and Cm determine the excitability properties of an excitable cell. RMP determines the number of available Nav, Cav and Kv channels by controlling the degree of inactivation of these channels, while Rm and Cm determine the effectiveness of current stimuli to excite a cell. Therefore, we first consider those properties of our RVMCs under our standard-normal conditions, including the variabilities of these properties.

The RMP recordings were rather stable around –70 mV (see Table 1). Initially, RMP values (RMPi) were around –60 mV (range –40 to –71 mV), but after a few minutes these values stabilized to an RMP=-69.5 $\pm$ 2.4 mV (n=20) and remained near that value for at least 15 min (see Table 1). A RMP of ~-70 mV, not far above the calculated Nernst potential for the K^+ gradient (-84 mV), is consistent with a major role of Kir-channels in establishing RMP.

Rm was measured in current-clamp with depolarizing 50- or 100-pA current pulses from RMP as well as with 10-mV depolarizing voltage-steps in voltage-clamp from a holding potential Vh= –60 mV: Rm(rmp)= 111$\pm$67 MΩ (n=17), while Rm(-60)= 384$\pm$296 MΩ (n=20) (Table 1) for the selected cells (criterium Rm(-60)>100 MΩ), consistent with an RMP mainly resulting from activation of *Ikir*-channels.

Cm-values were obtained from capacitive current responses to 10-mV depolarizing voltage-clamp steps and were Cm= 173$\pm$65 pF (n=20) (Table 1). Thus, the membrane time constant of the cells around RMP was ~20 ms (Rm(rmp).Cm), implicating latency times around 20 ms for AP-generation with just-above threshold current stimuli, consistent with the records in Fig. 1b and 2b.

The measurements imply a variability, in which RMP is remarkably constant between myocytes with a variation coefficient of 3%, compared to coefficients of Rm(rmp), Rm(-60) and Cm of 60%, 77% and 38%, respectively.

Group-1 RVMCs with High-peak/Long-duration pulse-evoked action potentials (HL-APs)

The differences in AP-properties between example group 1, group 2 and the remaining cells with intermediate properties enabled us to analyze current-clamp behaviour (excitability) in terms of voltage-clamp properties for groups of RVMCs with different excitability.

The first example of excitability is that of a myocyte with a high-peak (at +38mV) and long-duration AP (70-100ms at half height) (HL-AP) evoked by a short current pulse from a resting membrane potential RMP~-72 mV (Fig. 1b, c). The fast depolarizing and slow delayed repolarizing phase gives the typical asymmetrical shape of a mammalian cardiac AP with plateau-phase. Five out of 13 cells had APs of the HL-AP type further described below, i.e. with APPs of 30-40 mV and APDs of 50-110 ms at half-height (encircled as a group in the upper left corner of Fig. 4a).
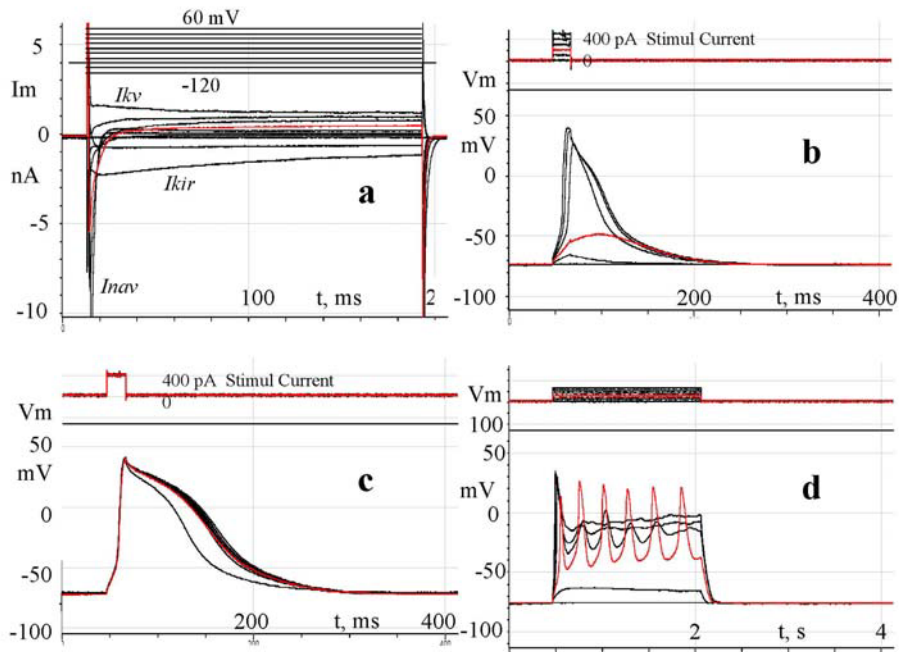
Fig. 1. Voltage- and current-clamp properties of an adult rat right ventricular myocyte (RVMC) with a high-peak and long-duration current-pulse evoked action potential (group 1 with HL-APs). All records are from the same cell.

(a) Superimposed voltage-clamp current-records from the cell evoked by voltage steps of 180 ms duration from the holding potential Vh=-80 mV to membrane potential (Vm) values of –120 mV and higher up to +60 mV, with increments of +20 mV. The resting intervals between the steps (at Vh=–80 mV) were 5 s. The voltage activated inward (negative) fast sodium current (*Inav*) is large compared to the maximal currents of the inward rectifier potassium current (*Ikir*) and the voltage-activated (positive) potassium current (*Ikv*). The short current peaks preceding the *Ina*, *Ikv* and *Ikir* records are the rapid capacitive current transients charging the membrane capacitance to the applied potentials. The initial resting potential (RMP) was –68 mV but stabilized later between –72 and -76 mV. Seal resistance (Rseal) was 6 GΩ, membrane capacitance (Cm) was 150 pF, membrane resistance at –60 mV (Rm(-60mV)) was 400 MΩ, and series resistance (Rser) was 5 MΩ.

(b) Superimposed Vm records (bottom records) upon short (20 ms) current-pulse stimulations with increasing intensities (0 to 500 pA, with 100-pA increments, see top records). Resting interval between the pulses was 5 s. Notice that the Vm-threshold for evoking an AP is ~-50 mV, while the current threshold is just above 100 pA. The first evoked AP is a bit shorter in duration than the two subsequent APs. The small instantaneous voltage changes in the records (order of 1 mV, consistent with an Rser=5MΩ) at the start and stop of the pulses are the voltage changes over Rser, which are also visible in Fig. 1c and 1d.

(c) Superimposed action potential (AP) records (bottom records), evoked by a 10-pulse/1-Hz train of 20-ms/400-pA current-pulses (top records). The shortest AP is the first AP, the 9 subsequent longer APs show some variation in repolarization time. Thus, the AP of this cell has largely adapted its APD to the train after ~1 s.

(d) Superimposed Vm records (bottom records) upon sustained depolarizing current stimulation with current steps of 1.6-s durations and increasing amplitudes with 50-pA increments from 0 to 250 pA (top records). Resting intervals between the current steps were 5 s. Notice that the amplitude and the number of waves in the damped oscillations decrease with increased current induced depolarization.

180

The voltage-clamp currents (Fig. 1a), evoked by voltage steps from a holding potential Vh=-80 mV,   show various current types. First, a sustained inward-rectifier K$^+$ current (*Ikir*; sustained over 180 ms with some degree of inactivation in this case) upon voltage steps downward to –100 and –120 mV. Second, a large and fast voltage-activated, transient inward Nav-current (*Inav*) upon steps to ≥-40 mV. The first signs of *Inav*-activation are visible upon a depolarizing step to –60 mV, while maximal *Inav* occurs at –40 mV with an *Inav*-peak current (*Inavp*) more negative than -10nA. Small sustained (over 180 ms) outward currents are visible at Vm-steps to >-20 mV and are considered here as Kv-currents (*Ikv,* mainly the sustained *Iss*), based on Pandit *et al.* (2001, 2003). Thus, in absolute value, the maximal *Inavp* is here much larger (>~5x) than the absolute value of the maximal inward-rectifier K$^+$ peak current (*Ikirp*=-2.4 nA at –120 mV) and the maximal voltage activated (outward-rectifier) K$^+$ current (*Iss*~+1.5 nA at +60 mV). A small inward L-type voltage-activated calcium current (*IcaL*) must be present in the whole-cell currents (Pandit *et al.*, 2001) but cannot easily be recognized under these standard recording conditions, because it is masked by *Inav* and *Ikv* (see Fig. 5). Furthermore, the outward currents do not show a prominent transient *Ikv, It*, as in the second example of a normal RVMC below. For an I-V curve representing the three main current components of this cell (*Ikir, Lnav* and *Iss*) see Fig.3.

Fig.1b shows the excitable behaviour of the selected RVMC upon application of short (20ms) current pulses of increasing amplitude from 0 to 500 pA. For such a pulse-evoked AP (pAP), the firing threshold of the membrane potential was around –50 mV at ~200-pA stimulation, consistent with activation of *Inav* at ~-50 mV in our voltage-clamp recordings (Fig.1a) and with the literature (Pandit *et al.*, 2001). pAP depolarization accelerated with earlier threshold crossing by the stronger pulses, while the pulse-evoked action potential duration (pAPD at half height) increased by a decelerated repolarization at the stronger pulses.

Since APD often depends on the rate of AP firing (Pandit *et al.*, 2001), APD was measured in a train of 10 APs (tAPs) evoked with supramaximal pulses (~2x the threshold current pulse amplitude) at a frequency of 1 Hz (Fig. 1c). Supramaximal stimulation was evident from the constantness of the peak amplitudes of the tAPs (tAPP=38 mV) and the absence of latency fluctuations. Fig. 1c shows indeed rate adaptation of tAPD to the train of 1 Hz by a significant tAPD increase after the first (shortest) tAP. This increase was not necessarily monotonic in a 1-Hz train. tAPD at 50% AP height of the 1st AP (tAP1D50) was 70 ms and increased to tAP10D50=90 ms at the 10th pulse after an overshoot of tAPD50max=100 ms. The mean tAP1P, tAP1D50 and tAP1D50max of the 5 HL-APs were 33 mV, 70 ms and 92 ms, respectively.

Depolarizing-current induced automaticity in the HL-AP group

A peculiar type of RVMC excitability was seen as repetitive AP firing upon depolarizing the cell with a sustained (1.6-s lasting) current. This depolarizing-current induced automaticity (DIA) is shown in Fig. 1d. DIA occurred in all RVMCs tested (n=18), was usually transient in nature (damped membrane potential oscillation), and was critically dependent on the degree of current-induced depolarization. The highest tendency to fire APs occurred at the lowest possible

depolarization just above –50 mV. Fig.1d shows that the higher depolarizations (at the higher sustained currents) cause stronger damped oscillations with fewer and smaller-amplitude APs or membrane potential waves. The oscillation at the lowest current amplitude (100 pA) occurs in this cell at a frequency of ~3.1 Hz. It starts with an initial depolarization, which develops too slowly to reach the threshold for triggering a fast full-blown sodium-channel based AP, because the Nav-channels largely inactivate before becoming activated (cf. Pandit *et al.*, 2001 for the properties of Nav-activation and inactivation). Nevertheless, the current-induced depolarization proceeds by closure of the inward-rectifier channels until the higher L-type calcium-channel threshold is reached around –30 mV (Pandit *et al.*, 2001). Because these calcium channels do not appreciably inactivate during the preceding depolarization, they are able to generate a typical slow calcium AP, which repolarizes by calcium channel inactivation and presumably by activation of residual (not yet inactivated) Kv-channels (cf. Pandit *et al.*, 2001, for the CaL and Kv-activation and inactivation properties). The duration of the first spontaneous AP, sAP, for 18 cells is sAP1D50~88 ms (see Table 1), thus in the range of durations of HL-APs (50-110 ms). However, the AP cannot return to the normal Kir-channel determined RMP, because of the applied sustained depolarizing current. This return of the membrane potential (Vm) to values of –50 to –30 mV allows recovery from CaL-channel inactivation causing repeated CaL-channel activation and generation of a repeated AP (Pandit *et al.*, 2001). Thus, this mechanism is similar to that of early afterdepolarizations (EADs) in the repolarizing phase of APs in ventricular myocytes of hypertrophic and failing hearts or from LQT-syndrome hearts (Rudy, 2000; Antzelevitch *et al.*, 2000). Therefore, the DIA may be seen as a series of repetitive EADs in normal heart cells.

Interestingly, DIA shows that Cav-channel excitability may be uncoupled from Nav-channel excitability in the slow onset of DIA and maintained during DIA when AP-firing continues above –50 mV, where all Nav-channels are inactivated (Pandit *et al.*, 2001; cf. Fig. 5b). At one higher applied current amplitude (150 pA), depolarization occurs fast enough to trigger an *Inav*-initiated AP as in Fig. 1b or c, but repolarization cannot be completed because of the sustained current, so that repeated APs can occur at the same frequency (~3.1 Hz) as at 100 pA, but with lower and sooner declining amplitudes and from a higher depolarized Vm~-30 mV, where more average CaL-channel inactivation occurs (Pandit *et al.*, 2001). A one-step higher depolarizing current (200 pA) shows such a strong damping of Vm-oscillation, that only one significant small wave is generated after the initial normal AP from a depolarized level of ~-25 mV. At 250 pA the after-oscillation of the initial AP from a depolarized level of –20 mV is almost completely suppressed.

The average number of spontaneous APs or waves in the DIA during the 1.6-s sustained stimulation was 3.6 (range 2-6), a little higher than that in the general population (2.9, see Table 1).

182

Table 1. Electrophysiological properties of right ventricular myocytes of the adult rat.

	Average	SD	unit	n
RMPi	-60.8	7.3	mV	20
RMP	-69.5	2.4	mV	20
Cm	172.9	65.2	pF	20
Rm(-60)	384.1	296.3	MΩ	20
Rm(rmp)	111.2	66.8	MΩ	17
Inavp(-40)	-7.1	3.2	nA	20
Ikirp(-120)	-2.9	1.0	nA	20
Ikvp(60)	2.9	1.6	nA	20
Iss(60)	1.2	0.5	nA	20
Itp(60)	1.7	1.3	nA	20
Itp(60)/Cm	9.1	6.6	pA/pF	20
Tit(60)	46.8	5.6	ms	6
tAP1P	19.6	17.3	mV	13
tAP1D50	41.0	28.4	ms	13
tAPD50max	61.2	44.2	ms	13
sAP1P	20.6	11.0	mV	18
sAP1D50	88.3	37.8	ms	18
sAPMDP	-31.2	9.2	mV	18
#sAPs/Waves	2.9	1.6		18

Table 1. Electrophysiological properties of right ventricular myocytes of the adult rat.
RMPi, initial resting membrane potential (mV), measured within 1 min after whole-cell establishment.
RMP, stabilized resting membrane potential (mV), measured a few minutes after whole-cell establishment.
Rm(rmp), membrane resistance (MΩ) measured in current-clamp with a depolarizing 100-pA current step from RMP (~-70 mV).
Cm, membrane capacitance (pF), measured on-line in voltage-clamp with a 10-mV depolarizing voltage step from a holding potential Vh=-60 mV with the use of the pClamp-protocol MemTest.
Rm(-60), membrane resistance (MΩ) measured in voltage-clamp with a 10-mV depolarizing voltage step from a holding potential Vh=-60 mV (same protocol to measure Cm).
***Inavp*(-40)**, peak sodium current (nA), measured at –40 mV test potential.
***Ikirp*(-120)**, peak inward rectifier K^+ current (nA), measured at –120 mV test potential.
***Ikvp*(60)**, peak voltage-activated outward K^+ current (nA), measured at +60 mV test potential.
***Iss*(60)**, sustained voltage-activated outward K^+ current (nA), measured at +60 mV at t=180 ms, the time that the transient phase of *Ikv* is largely over.
***Itp*(60)**, the difference (nA) between *Ikvp*(60) and *Ikvs*(60).
***Itp*(60)/Cm**, *Itp*(60) normalized for variability in Cm.
Tit(60), the time constant (ms) of decay of *It* at the 60-mV test potential , measured as the time elapsed between the peak of *It* and *Itp*/e.
tAP1P, the peak amplitude (mV) of the first AP of a train of 10 APs, evoked by 20-ms supramaximal (>1.5 current threshold) current pulses at 1 Hz.
tAP1D50, the AP-duration at 50% AP-amplitude (APP-RMP) of AP1 of the 10-AP 1-Hz train of APs.
tAPD50max, the maximal AP50-duration (ms) of the 10-AP 1-Hz train of APs.
sAP1P, the peak amplitude (mV) of the first spontaneous AP after the initial current-step evoked AP or occurring at lower currents without an initial AP.
sAP1D50, the AP-duration (ms) at 50% AP-amplitude of sAP1.
sAP1MDP, the maximal (negative) diastolic potential (mV) after sAP1.
#sAPs/Waves, the number of spontaneous APs or waves during a 1.6-s sustained current stimulation, i.e. the broad APs or subsequent waves with >10-mV amplitude, measured from the interpolated MDPs after the APs/Waves, and occurring after the initial current-step evoked AP or occurring at lower currents without an initial AP.

Characteristic for all DIAs is a considerable gap between the maximal (-negative) diastolic potentials (MDPs) of the DIA-oscillations and the last preceding Vm-response in the protocol not giving rise to DIA (see also Fig. 2d). This must be due to depolarization-induced closure of the Kir-channels causing an abrupt increase in the membrane resistance and thereby an abrupt increase in the current-step induced depolarization, as shown in Fig. 6c.

In conclusion, we found and compared two types of current-evoked excitation in a subset (group 1) of our normal RVMCs. The first one is represented by the classical short-pulse evoked *Inav*-initiated and *IcaL*-extended HL-APs and the second one is represented by spontaneously occurring *Inav*-independent, apparently *Icav*-driven (see further evidence below) slow action potentials induced by sustained current stimulation.

Group-2 RVMCs with Low-peak/Short-duration pulse evoked action potentials (LS-APs)

Fig. 2 presents a quite different type of RVMC excitability: the cell has a strongly expressed *Ikv* combined with a low-peak/short-duration AP (LS-AP, see Fig. 2b,c), despite a relatively large *Inav* (*Inavp* at -40 mV $<$-10 nA, Fig.2a). Nevertheless, DIA is preserved (Fig. 2d).

The voltage-clamp records (Fig. 2a) reveal an increased size of *Ikir* and *Ikv*, compared to the example group-1 RVMC in Fig. 1a, but now there is a pronounced expression of the transient component of *Ikv*, *It*. This makes the peak of *Ikv* at 60 mV more than 2x larger than that in the group-1 example RVMC (Fig. 1a). The more pronounced *It* in this group and in two other cells of the population allowed us to measure the time constant of inactivation of *It* at +60 mV for 7 cells, which was ~47 ms (see Table 1). *Ikir* has similar properties as in Fig. 1a, but the peak amplitude is almost doubled and the inactivation at -120 mV is less pronounced. The doubling of *Ikir* and *Ikv* in Fig. 2 compared to those presented in Fig.1 must be largely due to variability between the cells because Cm in Fig. 2 is only 7% larger and Rser is only 8% smaller than in Fig. 1 (see Figure legends). Fig. 3 shows the I-V curve derived from the records in Fig. 2a with explanations below.

Analysis of the records in Fig. 2b gives a clue on the role if *It* in depressing and shortening the pAPs in group-2 RVMCs. A local response occurs upon a pulse of 300 pA (4th record from below) bringing Vm to a value around an increased firing threshold of ~-40 mV. The low-peak AP-responses to the subsequent pulses of increasing strength repolarize faster than the local response to the 300-pA pulse, which indicates that *It* has been activated during these pAPs. As the regenerative upswing of the pAP occurs relatively slowly, *It* is activated rapidly enough (Pandit et al., 2001) to antagonize excitation during the initial AP-development. Thus, the increased *It* expression appears to depress and shorten the AP in LS-AP myocytes around -70 mV.

The other three group-2 RVMCs showed a similar but more pronounced picture of reduced excitability. The pAPP-values were lower (-10 to 0 mV) and the APs were no longer all-or-nothing but rather graded responses, which repolarized earlier in the higher responses, consistent with progressive *It* activation at Vm>-30 mV (cf.

Fig. 2a). These responses looked rather aborted APs – through *It* activation- than depressed APs.

In one extra LS-RVMC the aborted AP with an APP=–10 mV and APD50=28 ms changed to a higher-peak and shorter AP (APP=12 mV and APD50=13 ms) when the RMP spontaneously hyperpolarized from RMP=-66 mV to –72 mV, indicating that the exact RMP-value around –70 mV is an important determinant of excitability. This observation was confirmed by similar effects of membrane hyperpolarizations evoked by steady current injections in 3 of the 4 LS-cells.
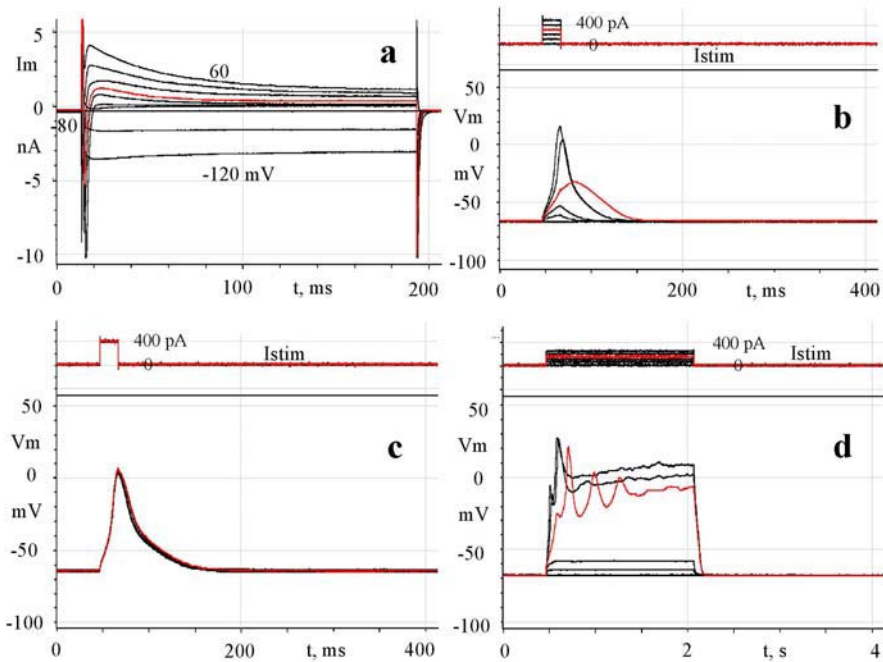
Fig. 2. Excitability of a group-2 RVMC with lowered and shortened pulse-evoked APs (LS-type) by strong *It* expression, but with preserved DIA.
(a) Voltage-clamp current records as in Fig. 1a. Notice the increased *It* expression compared with the HL-myocyte in Fig. 1a. The initial resting potential (RMP) was –60 mV but stabilized later between –65 and -68 mV (see Fig. 2b, c and d, with c preceding b in time). Rseal= 7 GΩ, Cm=161 pF, Rm (-60mV)=300 MΩ, Rser=4.6 MΩ.
(b) Vm records (bottom records) and applied-current records (top records) as in Fig. 1b. The APs have a low peak (0-10 mV) and short duration (LS-APs) compared to the APs in Fig. 1b, c. Notice a local response at liminal stimulation (3rd pulse) and that the subsequent APs upon the 4th and 5th pulse repolarize faster than the local response, indicating increased *Ikv*-activation by those pulses.
(c) AP-records and current-pulse records during 10-pulse 1-Hz stimulation as in Fig. 1c. Notice the practical absence of frequency adaptation of the LS-type AP compared to that of the HL-type AP (cf. Fig. 1 c).
 (d) Vm records and applied-current records to evoke DIA as in Fig. 1d. The Vm-oscillation is more damped than in Fig. 1d. Notice that a well-developed fast Nav-channel based AP is missing in the beginning of all records; but that slow Cav-channels based sustained-depolarization induced APs are present in the three upper records.

Reduced excitability around and above RMP=-70 mV is consistent with the inactivation curve of *Inav*, which shows already 80% inactivation at −70 mV, where inactivation of *It* is just beginning (Pandit *et al.*, 2001). Thus, the strongly increased *It* expression in LS-AP RVMCs depresses Nav-dependent excitability of these cells around −70 mV, which is in contrast to what happens in HL-APs (Fig. 1). Furthermore, the faster AP-repolarization upon steady hyperpolarizing LS-AP RVMCs from RMP>-70 to RMP<-70 mV must be at least partly due to making more *Iss* channels available by de-inactivation (Pandit *et al.*, 2001). Another striking difference between AP-properties of group-2 and group-1 myocytes is the absence of frequency adaptation in group-2 cells as shown in Fig. 2c.

DIA in the LS-AP group

The depressed AP with the accelerated repolarization would prevent the generation of the slower Cav-channel based APs, if these Cav-channels would be present in the cell.

Fig. 2d indeed shows that this group-2 RVMC has these calcium channels expressed because it is able to generate slow *IcaL*-based APs during DIA. In all 4 LS-type RVMCs the DIA was transient with 2 or 3 APs/waves. The occurrence of the slow APs after the initial depressed AP at the beginning of the higher current steps can be understood from the stronger and longer-lasting current-induced depolarizations counteracting the repolarizing influence of *It*-activation and allowing *It*-inactivation.

In summary, a relatively strong *It* is able to inhibit the *Inav*-based beginning of the action potential of group-2 RVMCs by starting a premature repolarization process. This premature repolarization then prevents the generation of the *IcaL*-based slower AP-component. Thus, APD regulation by *It*-controlled *IcaL*-activation implies, at least partly, *It*-controlled *Inav*-activation. However, during continuous current-induced membrane depolarizations to Vm>-40 mV *It* inactivates and can no longer prevent the occurrence of the slow spontaneous APs during DIA.

I-V relationships

In order to better illustrate the voltage-dependencies of the main currents of our right ventricular myocytes, we show in Fig. 3 current-voltage (I-V) curves of the two myocyte types, having HL- or LS-APs. The curves were derived from the voltage-clamp records in Figs. 1a and 2a (see legend for further information). The I-V curves show the increased expression in the LS-myocyte of *Ikv* (best measured at +60 mV), in particular of *It*, and the range of *Ikir* sizes for both cell types at voltages <-80 mV. Activation of *It* in the LS-cell occurs at Vm>-40 mV, consistent with Pandit *et al.* (2001). The absolute size of the maximal *Inav* at around -40 mV is only a rough underestimation of the real current size due to inadequate voltage-clamp conditions (too large Rser-values). Nevertheless, the curve reliably shows that *Inav* is activated at Vm>-60 mV, consistent with Pandit *et al.* (2001). *IcaL* is unrecognizable in the total whole-cell currents of the two cells plotted because of the presence of *Ikv*, but its presence can be revealed upon depolarizing voltage steps from een holding potential of –40 mV, as shown below in Fig. 5. For comparison, the I-V curve derived from that experiment has been

186

plotted in Fig.3 to illustrate how this hidden negative *IcaL* contributes to the total whole-cell current of a myocyte. The plot shows that *IcaL* activates in the same voltage range as *It*, consistent with Pandit *et al.* (2001). To visualize the real size of the outward (positive) *Ikv* current of a cell in the range of -40<Vm<60 mV, its negative *IcaL* (0 to −1.1 nA) should be subtracted from the total positive I-V curve in that Vm-range to obtain the real, more positive current of *Ikv*.
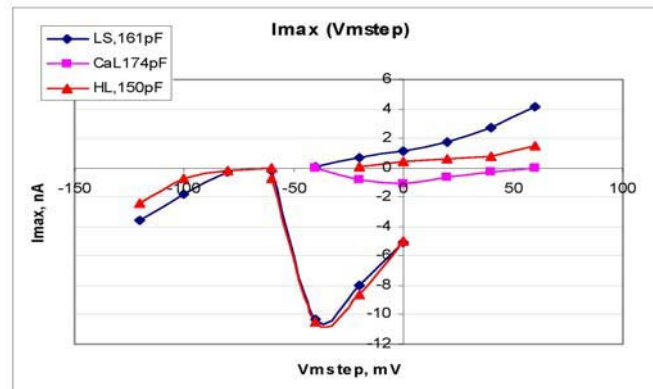
Fig. 3. I-V curves of the two types of myocytes with HL and LS-APs.
The curves consist of three unconnected parts, because the current amplitudes have been measured at different time points for different voltage ranges during the records. The left part (-120 to -80 mV) relates to that part of the I-V relationship representing maximal inward *Ikir*(Vm). The middle part (-60 to 0 mV) represents maximal inward *Inav*(Vm), while the right part (-20 to +60mV) represents maximal outward current, largely resulting from *Ikv*(Vm) . The latter current is, however, mixed with the inward current *IcaL*, which deforms the records except at +60 mV (~EcaL). For comparison, a *IcaL*(Vm) curve from another myocyte from the experiment of Fig. 5b has been added to the figure. All 3 cells plotted have comparable Cm-values (see legend in figure).

It affects pulse-evoked APs rather than DIA-APs

Comparison of Figs. 1-2 suggests that an increase in *It* expression lowers and/or shortens pulse-evoked APs, but not the initial DIA-APs, consistent with the idea that *It* is largely inactivated during DIA (cf. Pandit *et al.*, 2001). This hypothesis was tested by plotting and comparing the peaks and durations of the first APs in the short 1-Hz trains (tAP1P and tAP1D50; Fig. 4a,b) and of the first spontaneous APs during DIA (sAP1P and sAP1D50; Fig. 4c,d) as a function of the peak of *It*, measured at 60 mV (*Itp60*) and normalized to cell size by dividing *Itp60* by the membrane capacity Cm.
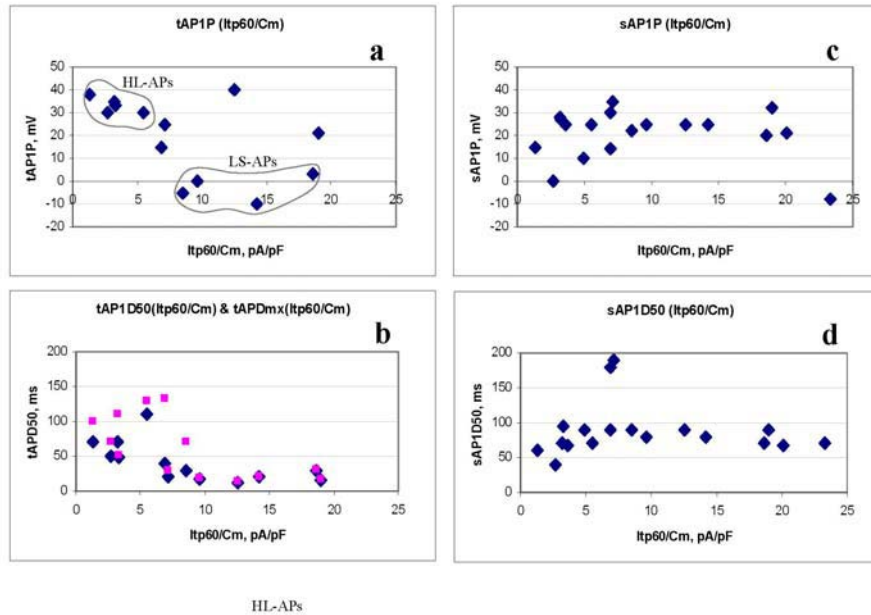
Fig. 4. The effect of *Itp,* normalized for cell-size (via Cm), at 60 mV on APP and APD for pulse-train evoked first APs (tAP1s, left frames, **a** and **b**) and for first spontaneous APs during DIA (sAPs, right frames, **c** and **d**) in the whole population. The two example-groups of myocytes with HL-APs and LS-APs are indicated in the figure. Notice the overall decline of tAP1P and tAP1D with an increase in normalized *Itp* and an absence of such a decline in the sAP1P and sAP1D values (for statistics see text). Notice also that the values of sAP1P and sAP1D are similar to the values of tAP1P and tAP1D at low normalized *Itp*-values. For definitions of the abbreviations, see the legend of Table 1.

The plots show lower tAP1P (Fig. 4a) and tAP1D50 (Fig.4b) values with an increase in *Itp60/*Cm (Spearman's correlation coefficient r_s=-0.569 and -0.817, resp.). This correlation is absent in the corresponding plots of sAP1P (Fig. 4c) and sAP1D50 (Fig. 4d) (r_s=0.003 and 0.168, resp.). tAP1 peaks decline from values ~30mV to values below 0 mV, while sAP1 peaks remain around 20 mV. Furthermore, tAP1 durations decrease from around 70 ms to values around 20 ms, while sAP1-durations remain high around 70 ms. This means that *It*-expression is an important determinant in APD regulation of pulse-evoked APs, but not in APD-regulation of DIA-APs. It also implies that, in general, the short pulse-evoked APs are not short as a result of a lack of *IcaL*-expression, as, if *It* inactivates under DIA-conditions, broad *IcaL*-based APs can appear. The location of the data points with the higher values of *Itp60*/Cm may need a right-shift because of underestimation of *Itp* due to imperfect voltage-clamp, but such a shift is not expected to affect the outcome of the used correlation test, because the Spearman test is based on rank correlation.

Fig. 4b shows another interesting property of pulse-evoked APs. They only show AP-lengthening in a 1-Hz train (frequency adaptation) for values of *Itp60*/Cm

188

below a certain value (~9pA/pF), i.e. for APDs already longer than the short APD (~20 ms) as observed at the higher *Itp60*/Cm values.

IcavL *measured under conditions of* Inav *and* Ikv-*inactivation*

To establish the expression of L-type Cav-channels in our myocytes under our experimental conditions, we recorded *IcaL* under the standard/normal conditions of the AP-recordings of Figs. 1-2 at a holding potential of Vh=-40 mV. At that potential the masking effect of other currents on *IcaL* is minimal, because *Inav* is completely inactivated, *It* largely and *IcaL* only slightly (cf. Pandit *et al.*, 2001).

Fig. 5 shows the results of such an experiment for a myocyte with properties intermediate between those of groups 1 and 2. In the control experiment of Fig. 5A it can be seen that *Ikir*, *Inav* and *Ikv* dominate the recordings at Vh=-80 mV, making *IcaL* invisible. However, *IcaL* is clearly recognizable at Vh=-40 mV in Fig. 5B, where *Inav* is completely and *It* is largely inactivated. *Ikir* is not much affected, as expected. The inactivation of *Inav* and *It* was largely reversible upon re-application of Vh=-80 mV (see legend of Fig. 5).
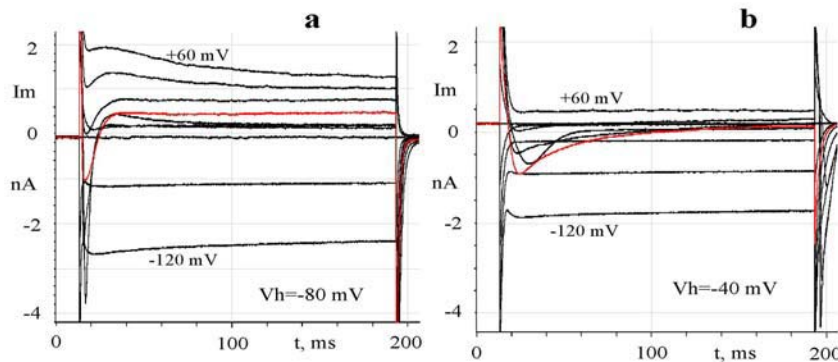
Fig. 5. Properties of *IcaL* measured under conditions of inactivation of *Inav* and *Ikv* for a RVMC with properties intermediate between those of groups 1 and 2.

(a) Control recordings of membrane currents at a holding potential Vh=-80 mV, showing voltage-dependent activation of *Ikir*, *Inav* and *Ikv* as in Fig. 2a. Conditions at the start of these recordings were: RMP=-71 mV, Cm=160 pF, Rm(-60)=160 MΩ, and Rser=12 MΩ.

(b) Membrane current recordings evoked as in (a), but from a Vh=-40 mV. At that Vh *Inav* is completely inactivated and *Ikv* largely, but *IcaL* only slightly. *IcaL* is first clearly evoked at –20 mV, is maximal at 0 mV, becomes smaller at more depolarized potentials and is zero at 60 mV. The inactivating effect of Vh=-40 mV on *Inav* and *Ikv* was largely reversible upon return of Vh to –80 mV (not shown here). *Inav* recovery was 57% and *Ikv* recovery 77%. *Ikir* did not recover, indicating a run down of the experimental conditions.

189

In this myocyte, *IcaL* activates above –40 mV, is maximal at 0 mV and reverses at +60 mV. The I-V curve of this current is plotted in Fig. 3 for comparison with the total current I-V curves of a HL and LS-cell. The peak amplitude at Vm=0 mV, *IcaLp(0)*, is –1.1 nA and this peak decays approximately exponentially with an inactivation time constant τicaL(0) of ~35 ms. The precise course of the I-V curve may be slightly different from the plot in Fig. 3 because of incomplete inactivation of *It* at –40mV.

Similar *IcaL*-properties were found in one other cell and are consistent with other studies (Clark *et al.*, 1993; Lee *et al.*, 1997).

DIA involves L-type calcium-channel based excitability

Given the literature about DIA in various rodents (cf. Katzung, 1975; Malecot *et al.*, 1985; Peters *et al.*, 2000) and about the properties of expressed ion channels in rat ventricular myocytes (cf. Pandit *et al.*, 2001, 2003), cardiac L-type calcium channels (Cav1.2) are the primary candidate for generating the spontaneous slow APs during DIA in rat RVMCs. They even may provide the pacemaker mechanism for current-induced automaticity, or at least contribute to it. Therefore, we have studied the effect of the cardiac CaL-channel (Cav1.2) blocker nifedipine on DIA. The concentration used was 10 μmol/L, because this concentration is supposed to inhibit almost 100% of the cardiac L-type Cav-channels at our resting membrane potentials of about –70 mV, without having disturbing aspecific effects on other channels (Hille, 2001).

Fig. 6 shows the results of such an experiment. The RVMC tested showed the three primary current types observed in the previous cell examples (*Ikir*, *Inav* and *Ikv*), but resembled more to group-2 RVMCs than to group-1 RVMCs, because *Ikv* had a clear *It*-component (Fig. 6a). This caused a smaller APP (~13 mV) than in group 1. Application of 10 μmol/L nifedipine completely abolished DIA (Fig. 6c). The same stimulus protocol now resulted in *Ikir* and *Ikv* dominated responses of Vm. *Ikir* closure upon depolarization was now evident from the gap in the responses between zero current stimulation and stimulation with 50-pA current. *Ikv* activation was evident from the abrupt stop in the time course of the current-step induced depolarization at voltages of –35 mV and higher. Inactivation of the *It* component is visible in the records at Vm values of –30 mV and higher as a delayed development of depolarization, consistent with the transient nature of *It* in the voltage-clamp responses in Fig. 6a. The survival in 10 μmol/L nifedipine of *Inav*, *Ikir* and *Ikv* with its *It* component is visible in Fig. 6d for a different cell, recorded in the solution of the cell in Fig. 6a-c after loosing that cell. The change in the precise initial time course of *Ikv* may be the result of the removal of the interference of *IcaL* with the recorded *Ikv* or due to non-ideal voltage-clamp conditions.

These effects have been found in total for 4 cells and are consistent with comparable experiments on DIA in cardiomyocytes of other mammals (Peters *et al.*, 2000). We conclude therefore that L-type calcium channels provide the inward currents for the slow APs in the DIA. A second conclusion is that both the *Ikir* and *Ikv*-channels in some way contribute to the occurrence and mechanism of DIA. Kir-channels contribute, because it is the depolarization-induced closure of Kir-channels which brings the cell in the DIA-mode and a lack of reactivation keeps

190

the cell in the DIA-mode. Kv-channels must contribute in some way to DIA, because they are being activated and inactivated in the voltage range in which the slow APs occur. One significant role of *It* turns out to delay DIA, when a slow depolarization develops (cf. Fig. 6b).
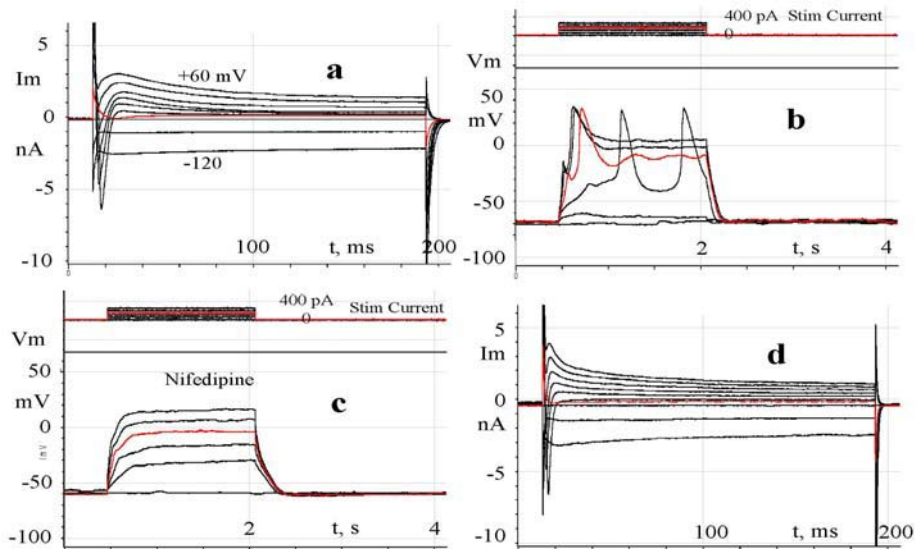
Fig. 6. The effect of 10 μmol/L nifedipine on depolarizing-current induced automaticity (DIA) of a RVMC with AP-properties (APP~13mV) between those of group 1 and 2. **(a)** Whole-cell voltage-clamp records, obtained as in Fig. 1a before addition of nifedipine. *Ikir*, *Inav* and *Ikv* with a *It* component are present. Rseal>1GΩ, Cm=233pF, Rm(-60mV)=152MΩ, Rser=7MΩ. **(b)** DIA with slow APs, evoked from RMP=-70 mV. Records taken before the addition of nifedipine. The DIA inducing current steps were too small to evoke an initial full-size AP. **(c)** Vm responses upon the same stimulus protocol as in (b), after the addition of 10 μmol/L nifedipine. RMP was decreased to ~ -60mV. **(d)** Voltage-clamp records, obtained as in (a), but from another RVMC in the presence of 10 μmol/L nifedipine and serving as a voltage-clamp equivalent of the records in (c)

Exploring cardiomyocyte excitability mechanisms with a computer model

The main two questions studied were whether the model of Pandit *et al.* (2001, 2003) in its uncoupled membrane version of the RVMC is able to qualitatively reproduce (**1**) the changes in pAP-shape for different myocytes with variable It, as well as (**2**) the various types of DIA (weak and strong damping) observed in these cells. To answer these questions we ran simulation experiments with the model under conditions close to our experimental conditions (extra- and intracellular ion concentrations and Rser, see legends of Fig. 7 and 8).

Fig. 7 concerns the first question and shows that a small-It RVMC has a much wider pAP with a higher plateau-phase than a large-It (epicardial) RVMC,

191

consistent with our observations (Figs 1-2 and 4) and consistent with the concept of a mechanism in which the approximate simultaneous activation of It with IcaL (Pandit *et al.*, 2001; Fig. 3) after Inav-activation inhibits IcaL and its depolarizing effect on Vm. However, the large-It RVMC does not show strongly reduced pAPPs as in Fig. 2b,c or aborted pAPs as in group-2 RVMCs with pAPPs<0mV. The latter failure could not be repaired by decreasing Inav or increasing It with a factor of 5 suggesting that the kinetics of Inav- and Ikv-activation in the model is more separated in time than in the experiments, where Ikv-activation can even suppress the initially developing Inav-driven pAP, thus preventing a IcaL-driven second part of the AP. Frequency (0.5-5 Hz) adaptation of the AP (lengthening with higher pacing rate) was also produced by the model as a consequence of cumulative inactivation of *It* (not illustrated here).
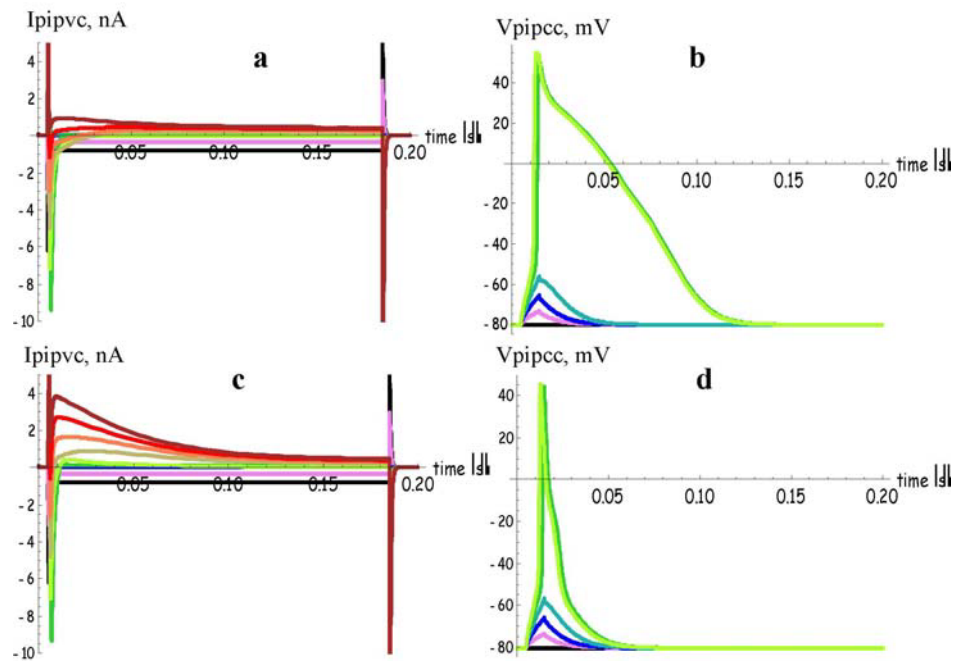
Fig.7. Correlation of It-expression in the model RVMC, as reflected in voltage-clamp simulation experiments (a, c), with pulse-evoked AP-shapes in current-clamp simulation experiments (b, d). The voltage-clamp and current-clamp simulations were carried out with a series resistance Rser=6 MΩ, the approximate average Rser value in the experiments. External calcium concentration was as in our experiments (1.8 mmol/L). Intra- and extracellular K^{+} and Na^{+} concentrations were close to our experimental values. Properties of the various ion conductances in the membrane of the epicardial RVMC in (c) and (d) were as in Pandit et al. (2003). To simulate a small-*It* myocyte of the experiments (a) and (b), only *It* of the default epicardial cell was changed to 0.23x of the default value. The electrical behaviour of the myocyte membrane was uncoupled from intracellular ion- and calcium-dynamics by keeping $[Ca^{2+}]$=79 nmol/L, $[Na^+]i$=10.7 mmol/L , and $[K^+]$ = 139.3 mmol/L.

192

A model myocyte with a high *It* and short AP (the default right epicardial model cell) had much less frequency adaptation at 2-5 Hz stimulation than that cell with a smaller *It* (e.g. 0.25x), consistent with the experimental result in Fig. 1b, 2b and 4b.

Fig. 8 illustrates the answer to the second question. An epicardial RVMC (with a large It) does not clearly exhibit DIA-behaviour when sustained-current stimulation with increasing intensities is applied (Fig. 8a). This can, however, be repaired by increasing Iss with a factor of ~4, allowing the generation of DIAs of 2 after-APs after the initial AP at intermediate stimulus intensities (Fig. 8b).
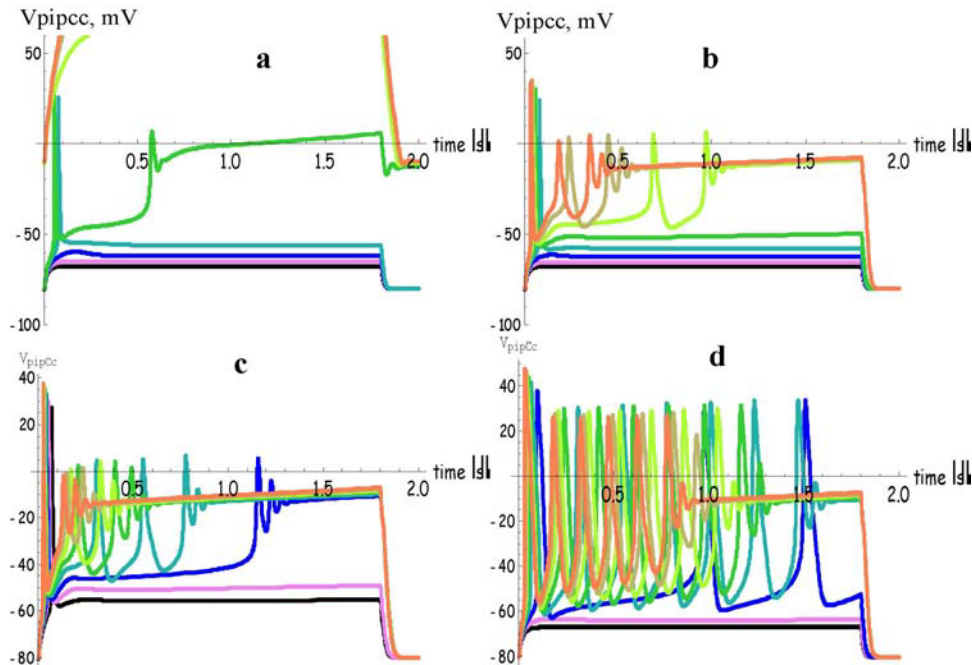
Fig. 8. Conditions required for the occurrence of DIA in the model of Pandit et al. (2001, 2003) of the RVMC of the adult rat (membrane uncoupled from the intracellular calcium dynamics). In all simulations $[Ca^{2+}]e$=1.8 mmol/L and Rser=6MΩ, as in our experiments. The stimulation protocol started with a 1.8-s 0.1-nA current stimulus which was repeated with 5-s intervals (to obtain 8 records) and with current increments of 0.01 nA. Panel (a) shows the behaviour of the default epicardial RVMC (see Pandit et al. 2003) unable to generate DIA. After increasing Iss with a factor of 4, the cell is able to generate DIAs at intermediate stimulation intensities (b). Reducing Ikir with 1/3 in panel (c) further facilitates DIA in the model cell of panel (b). In panel (d) It of the cell in panel (b) is reduced to 10%, causing a longer lasting DIA with broader and higher-amplitude APs.

A strong right-shift of the inactivation curve of *Iss* has a similar effect. Additional simulations (not shown here) revealed that these sustained-stimulation induced

APs survive the removal of Inav, disappear after removal of IcaL (consistent with the experimental result of Fig. 6) and are not or only slightly affected by the removal of If, Icap, Ib, Inaca and Inak. Thus, the induced APs are IcaL-driven and require sufficient Iss expression. Increasing the time constant of inactivation of *Iss* turned out to increase the number of APs in the DIA-transient. Removal of the window current of IcaL bij shifting the inactivation curve of IcaL 10 to 15 mV to the left (not shown here) removes the sustained-current induced APs, indicating that the automaticity mechanism resides in the overlap of the activation and inactivation curve of IcaL. However, other K$^+$ currents than *Iss* are also important in the generation of DIA. Fig. 8c shows that reduction of Ikir facilitates the occurrence of DIAs, because they occur at lower stimulation currents with more APs (less damped oscillation).

Finally, It seems to have an inhibitory effect on the DIAs, because reduction of It to 10% of the default value (Fig. 8d) makes the initial AP and subsequent ones broader and of larger amplitude and makes the train of induced APs longer (weakly damped oscillation).

These results imply that the variable DIA-phenotype observed in our experiments can be qualitatively reproduced from variable combinations of the main membrane currents playing a role in this phenomenon, IcaL, Iss, Ikir and It. Thus, in principle, the mechanism of DIA resides in the membrane and does not require a connection of the membrane with the intracellular calcium (and other ion) dynamics. Naturally, such a connection can be expected to serve as an important regulator of DIA, for example because intracellular calcium can control IcaL through calcium-induced inactivation (cf. Antoons *et al.*, 2007), a mechanism included in a simple form in the complete model of Pandit *et al*. (2001, 2003).

A preliminary analysis of these results in terms of gating behaviour of the ion channels involved (not shown here) indicates that the automaticity mechanism of DIA resides in the window-current properties of IcaL in combination with the deactivation properties of Iss. DIA requires AP-repolarization towards a membrane potential within the window current range to allow de-inactivation of IcaL to provide 'diastolic' depolarization by inward *IcaL*, which is then supported by 'diastolic' deactivation of Iss to recover from activation during the preceding action potential. The strength of sustained stimulation in combination with the presence of other active currents, Ikir, It and the sum of the smaller currents, determine whether the membrane potential can land after the first AP in the window current range of the membrane potential. The slow inactivation of Iss may then determine the length of the AP-train of the transient DIA. The differences regarding the phenotype between the DIAs of the different RVMCs of the heart may thus result from the variability in the expression of the various ion channels.

194

Discussion

The principal findings of the present experimental and model study concern **(1)** the role of the transient K$^+$ current *It* in RVMC action potential (AP) shaping, and **(2)** the roles of *Ikv* (*It* and *Iss*) and *Ikir* (inward-rectifier K$^+$ current) in depolarizing-current induced automaticity (DIA).

It controls AP-duration by controlling *Inav* as well as *IcaL*-activation

Under our conditions, the transient current *It* turned out to control the shape of current-pulse evoked APs, by starting an initial repolarization process as soon as the *Inav*-initiated depolarization phase of the AP surpasses the activation potential of *It* around –30 mV (see our voltage-clamp currents and Pandit *et al.*, 2001). If *It* would be absent, the AP would develop an *Inav*-driven AP lasting long enough to allow activation of the *IcaL* around –30 mV. *Inav*-inactivation would then automatically remove the depolarizing influence of the Nav-channels. This influence is then replaced by that of the CaL-channels to generate the cardiac AP-plateau and lasts as long as *IcaL*-inactivation and activation of residual *Ikv* (*Iss)* and background currents allow the CaL-channels to remain active. This situation approximates the conditions in the myocytes with HL-APs, where no or relatively little *It* is present, but some *Iss*. If enough *It*-channels are present, they limit *Inav* by activation above –30 mV and thereby the degree of depolarization by *Inav*. At the same time the *It*-channels provide a hyperpolarizing force, against which *IcaL*-channels have to become activated. This limits the number of activated CaL-channels and the degree of depolarization these channels can contribute to the membrane. Thus, *It*-channels have a double-negative influence on CaL-channel induced membrane-depolarization during the AP, the first being hindrance of *Inav*-induced depolarization and the second being hindrance of the depolarizing action of already-open CaL-channels. In this way, CaL-channel activation, and consequently APD, can be controlled by *It*-channels*.* In the extreme case, as in group-2 APs, *It* can be so strong, that it even aborts an *Inav*-driven AP thereby also preventing *IcaL*-activation. In a functional myocyte, this would also mean electro-mechanical uncoupling.

This concept of the role of *It* in cardiomyocyte excitability applies to our preparation of rat RVMCs with their RMP~-70 mV, which is 5-10 mV more positive than reported by others (cf. Pandit *et al.*, 2003). This seems the reason that our simulation experiments with the model of Pandit *et al*. (2003) did not reproduce the depressed and aborted APs in the high-*It* cells (see below). At the more negative RMP=-80 mV *Inav* is largely de-inactivated (Pandit *et al.*, 2001). At that potential the increased *It* expression in the LS-cells is no longer expected to affect APP, but only APD, as shown in our simulations with the Pandit model.

The above formulation of the mechanism of the regulation of APD by *It* follows from a careful comparison of current-clamp responses to voltage-clamp responses of the same cell under the same standard-normal conditions for diverse cases (from HL- to LS-APs). It may not be entirely novel, but an explicit formulation of this mechanism is required for a proper evaluation of changes of

ion channel expression during heart-failure associated remodeling of ion channel expression.

Kir-, CaL- and *Kv*-channels in the automaticity mechanism of DIA

The experimental results show that DIA may occur in rat ventricular myocytes and indicate that *IcaL* and *Ikir* are important components in the automaticity mechanism. Preliminary observations indicate that DIA may also occur in left ventricular myocytes of the rat (not shown here). Closure of Kir-channels by current-induced depolarization may bring Vm in a voltage range where a *IcaL*-driven pacemaker ('automaticity') mechanism can arise based on the overlap of the activation and inactivation curves of *IcaL* in these cells (Pandit *et al.*, 2001). In this mechanism (see Ishikevich, 2005) the 'diastolic inward pacemaker current' would result from recovery of *IcaL*-inactivation in a voltage range where a fraction of the activation gates is still open. However, Kv-channels may also participate in this automaticity mechanism, but the observed slowly inactivating Kv-channels (Kss) are a more likely candidate than the rapidly inactivating Kv-channels (Kt; see for the inactivation properties of Kt and Kss, *Pandit et al.*, 2001). A minor role for *It* is consistent with our observation that a rapidly inactivating Kv can only transiently suppress and thereby delay DIA. The role of Kss could then be to make DIA transient of nature by slowly inactivating (over the course of a few seconds) after the onset of DIA. Obviously any other repolarizing or depolarizing background or voltage-dependent current would also contribute to the automaticity mechanism. Our model simulations indeed revealed that *Iss* is an important participant in the automaticity mechanism of DIA (see below). Our view on *IcaL* as a 'diastolic pacemaker current' in DIA and on the accessory roles of Kv-channels in the generation of DIA is consistent with earlier interpretations of DIA-mechanisms described by Peters *et al.* (2000).

Origins of variability

The variability in expression of *It* between the myocytes was obvious from the initial overshoot of *Ikv* (*Ikvp*) over the sustained *Ikv* (*Iss*, see Figs. 1a, 2a). The origin of this *Ikvp* variability may be assumed to reside largely in the variable histological (endo-, meso- and epicardial) origin of the cells (Clark *et al.*, 1993). The variability of *Ikv* below 60 mV may be influenced by variability in the expression of *IcaL* (Lee *et al.*, 1997), which current is present (though unrecognizable) in our whole-cell total current recordings (Fig. 5). How this *IcaL* variability affects *Ikvp* variability remains to be determined in pharmacological experiments. Rser-variability is another source of variability affecting the higher *Ikvp*-values around 5nA at +60 mV.

A possibly important source of variability to be mentioned is the variability in Rm between the cells and within the cells in the course of an experiment. This variability affects RMP, excitability for current pulse stimulation, as well as inducibility of DIAs. The origin of Rm-variability is yet unclear, but may include variability in Rseal, in the expression of small unidentified membrane conductances and in cytoplasmic factors affecting ion channel function.

196

Besides *Ikv* variability we found variable *Inav* and *Ikir* values. Although *Inav* may be expected to be variably expressed in our cells (Pandit *et al.*, 2001), we did not quantify this variability, because of inadequate voltage-clamp conditions (too high Rser values) for this purpose. We neither studied here *Ikir* variability, because our focus was primarily on the role of *Ikv* in action potential generation and depolarizing-current induced automaticity. However, the role of *Ikir* in both excitability phenotypes remains of interest because of its repolarizing role in pulse evoked action potentials and its permissive role in DIA.

Differences with other studies

Although our results with respect to the expression of the main ion channel types (Kir, Nav, CaL and Kv) generally agree with findings of others who studied adult rat RVMCs (see Pandit *et al.*, 2001), there are a few differences. For example our RMP is 5-10 mV more positive than reported by others (Lee *et al.*, 1997; Pandit *et al.*, 2003), while the APDs are often larger (e.g. 42 ms compared to 14 ms). The first difference, the slightly depolarized condition, may certainly explain a large part of the increased APDs, because APD is sensitive for depolarization above –80 mV, probably mainly due to inactivation of Kv-channels causing diminished repolarizing force (Pandit *et al.*, 2001). Preliminary results showed an average APD-increase of 2-3 ms per mV depolarization over the membrane potential range –80 to –40 mV. The reason of the slight depolarization of the resting membrane is unclear but may be due to a difference in experimental conditions.

Another difference is a larger Cm (~172 pF) than measured by others (e.g. ~90 pF in Lee *et al.*, 1997). This difference may result from several causes, including opposite differences in bias at the selection of cells or in the method of Cm measurement. Future experiments should evaluate these differences.

Model results

The simulations with the model of Pandit *et al.* (2001, 2003) in its cytoplasma-uncoupled membrane version qualitatively reproduced the experimentally observed dependency of AP-duration on *It* and that of DIA on *IcaL* and the strength of the depolarizing current, while the participation of *Iss* was a new finding for the model DIA-behaviour. However, we are still far from a quantitative reproduction of AP-shapes in pulse-evoked APs and in repetitive AP-firing induced by sustained current stimulation. Depressed and aborted pAPs were not reproduced and DIA-reproduction required an increase in *Iss*, despite the fact that DIA was a regular finding in almost all cells. Fixing these problems would require a careful inspection of the exact activation and inactivation kinetics of Inav, *IcaL*, *It* and Iss. These limitations of the model indicate that the model of Pandit *et al.* needs updating of its membrane conductance properties with more detailed voltage-clamp measurements, which may already be available in the recent literature. An example of a further improvement of Pandit's model for a better understanding of frequency adaptation of the ventricular myocyte AP is found in Salle *et al.* (2008). For the DIA the precise de-inactivation properties of *IcaL* and de-activation properties of *Iss* are of crucial importance, because these currents appear to provide the automaticity mechanism of the DIA. However, the currents *Ikir* and *It* also need to be determined precisely because *Ikir* is permissive in

allowing DIA to occur, while *It* has both fast and slow components, which both may affect DIA, the fast component in initially inhibiting DIA and the slow component in contributing to DIA in a similar way as *Iss,* e.g. in making DIA transient.

The reproduction by the model of the experimental finding that frequency adaptation is much more pronounced in small-*It* myocytes (see Fig. 4b) is of functional interest. Frequency adaptation may be considered as being largely due to cumulative inactivation of *It* (Salle *et al.*, 2008). This would imply that small-*It* (non-epicardial) myocytes (i.e. with large AP-durations) would be more sensitive to cumulative *It*-inactivation and would be more inclined to develop pathogenic AP-lengthening at high heart rates.

To our knowledge, this is the first time that the classical phenomenon of depolarizing-current induced automaticity, described since Katzung (1975) and later also by others in ventricular myocytes in various species of mammals, has been analyzed with the use of a quantitative membrane excitability model. The results indicate that this type of analysis may increase our understanding of the mechanism of abnormal automaticity of myocardial tissue.

Functional implications

The mechanism described above for the effect of *It* on APD may have a wider meaning than only for heart failure-related APD changes in the rat heart, since *It* is also important in shaping the human cardiac AP (Beuckelmann *et al.*, 1993). So far, emphasis in shaping the human cardiac AP was more on the slower acting *Ikv's ,* such as *Ikr* and *Iks*, controlling APD by cutting off the terminal phase of the AP-plateau (Sanguinetti & Tristani Firouzi, 2006) instead of controlling APD by simultaneous inhibition of *IcaL* by *It* (see I-V curves in Fig. 3), as described here for the rat. An exception in this respect is the study of Greenstein *et al.* (2008), which ascribes an important role to *It* in controlling APD in canine ventricular cells

As described, we observed depressed and aborted APs in high-*It* myocytes with a 5-10 mV depolarized RMP~-70 mV (compared to the literature). This implies that areas of intact myocardial tissue of cells with increased *It*, such as epicardial cells, can become inexcitable when the membrane becomes 5-10 mV depolarized by whatever reason (hyperkalemia, ischemia). This would introduce heterogeneity in the tissue, allowing reentry and the development of ventricular arrhythmias. Down-regulation of *It* in hypertrophic and failing hearts, at risk of becoming locally depolarized by inadequate perfusion, may thus be seen as an adaptive response protecting the tissue against the development of abnormal heterogeneity in excitability.

The mechanism described for DIA may also have a wider meaning than for the rat heart alone. This mechanism may underlie DIA as well as EAD in greater mammalian species. Although the EAD-mechanism has been sought for in the properties of CaL-channels (Antoons *et al.*, 2007), studies so far have not pinpointed that mechanism to the intrinsic pacemaker properties of CaL-channels originating from the overlap between their activation and inactivation curves, which seems to apply to all mammalian ventricular myocytes. This may explain why EADs have the tendency to occur repetitively (Pogwizd and Bers, 2004). The

similarity between DIA and the Vm-oscillations during Torsade de Pointes (TdP) arrhythmias (Antzelevitch *et al.*, 2000) suggests that the automaticity-mechanism of DIA may also underly or contribute to TdP and in this way be responsible for the risk of sudden death in patients with long QT-intervals.

Perspective for Experimental Pulmonary Hypertension

The present study provides the control electrophysiological properties of adult rat RVMCs for a comparative study with RVMCs obtained from adult rats with experimental pulmonary arterial hypertension (PAH; cf. Lee *et al.*, 1997 and this thesis). Our results show great variability in excitability and ion channel expression, in particular of *It*, in adult rat RVMCs, probably arising from the precise histological origin of the cells from the right ventricle. In a preliminary electrophysiological study of RVMCs from rats treated with monocrotaline to induce PAH, we observed the same kind of variability as described here for control cells: HL-, LS- and intermediate types of action potentials were found in current-clamp and a similar variability of *It* expression in voltage-clamp experiments.. Establishing statistical differences between these groups would require large groups of observations. Thus, it would be easier to establish statistical differences between the electrophysiological properties of control and PAH-cells by comparing subsets of cells of the same origin from the tissue, for example cells of mainly epicardial, mesocardial or endocardial origin (cf. Clark *et al.*, 1993). Variability remaining despite such a procedure could then be evaluated in plots such as Figs. 4.

The present results suggest to consider two possible roles of Kv-channel expression in the arrhythmogenicity of cardiac tissue of the hypertrophic and failing heart. One is the role of Kt-channel expression in creating inexcitable areas in the tissue (reentry) upon the occurrence of small depolarizations (~10 mV) and the other is the role of Kss-channel expression in the automaticity response of the tissue (ectopic beats) upon the occurrence of larger depolarizations (~40 mV).

Acknowledgement

199

References

1. Antoons G, Volders PG, Stankovicova T, Bito V, Stengl M, Vos MA, Sipido KR. Window Ca^{2+} current and its modulation by Ca^{2+} release in hypertrophied cardiac myocytes from dogs with chronic atrioventricular block. J Physiol 2007;579:147-60

2. Antzelevitch C, Yan G, Shimizu W, Burashnikov A. Electrical heterogeneity, the ECG, and Cardiac arrhythmias. In: Zipes and Jalife, Cardiac electrophysiology from cell to bedside, 3rd edition, W.B. Saunders Company, Philadelphia, PA, USA, 2000.

3. Beuckelmann DJ, Nabauer M, Erdmann E. Alterations of K^+ currents in isolated human ventricular myocytes from patients with terminal heart failure. Circ Res 1993;73:379-85

4. Cerbai E, Barbieri M, Li Q, Mugelli A. Ionic basis of action potential prolongation of hypertrophied cardiac myocytes isolated from hypertensive rats of different ages. Cardiovasc Res 1994;28:1180-7

5. Clark RB, Bouchard RA, Salinas-Stefanon E, Sanchez-Chapula J, Giles WR. Heterogeneity of action potential waveforms and potassium currents in rat ventricle. Cardiovasc Res 1993;27:1795-9

6. Greenstein JL, Wu R, Po S, Tomaselli GF, Winslow RL. Role of the calcium-independent transient outward current $I_{(to1)}$ in shaping action potential morphology and duration. Circ Res 2000 ;87 :1026-1033

7. Guo D, Zhao X, Wu Y, Liu T, Kowey PR, Yan GX. L-type calcium current reactivation contributes to arrhythmogenesis associated with action potential triangulation. J Cardiovasc Electrophysiol 2007;18:1-8

8. Hille B. Ion channels of excitable membranes, 3rd edition, Sinauer Associates, Inc. Publishers Sunderland, MA, USA, 2001.

9. Ishikevich EM. Dynamical systems in neuroscience: The geometry of excitability and bursting. The MIT Press, Cambridge, MA, USA, 2005.

10. Katzung BG. Effects of extracellular calcium and sodium on depolarization-induced automaticity in guinea pig papillary muscle. Circ Res 1975;37:118-27

11. Lee JK, Kodama I, Honjo H, Anno T, Kamiya K, Toyama J. Stage-dependent changes in membrane currents in rats with monocrotaline-induced right ventricular hypertrophy. Am J Physiol Heart Circ Physiol 1997;272:H2833-H2842

12. Malécot CO, Arlock P, Katzung BG. Amrinone effects on electromechanical coupling and depolarization-induced automaticity in ventricular muscle of guinea pigs and ferrets. J Pharmacol Exp Ther 1985;232:10-9

13. Oudit GY, Kassiri Z, Sah R, Ramirez RJ, Zobel C, Backx PH. The molecular physiology of the cardiac transient outward potassium current (I(to)) in normal and diseased myocardium. J Mol Cell Cardiol 2001;33:851-72

14. Pandit SV, Clark RB, Giles WR, Demir SS. A mathematical model of action potential heterogeneity in adult rat left ventricular myocytes. Biophys J 2001;81:3029-51

15. Pandit SV, Giles WR, Demir SS. A mathematical model of the electrophysiological alterations in rat ventricular myocytes in type-I diabetes. Biophys J 2003;84:832-41

16. Peters NS, Cabo C, Wit AL. Arrhythmogenic mechanisms: Automaticity, triggered activity, and reentry. In: Zipes and Jalife, Cardiac electrophysiology from cell to bedside, 3rd edition, W.B. Saunders Company, Philadelphia, PA, USA, 2000.

17. Pogwizd SM, Bers DM. Cellular basis of triggered arrhythmias in heart failure. Trends Cardiovasc Med. 2004;14:61-6

18. Rudy Y. Ionic mechanisms of cardiac electrical activity. In: Zipes and Jalife, Cardiac electrophysiology from cell to bedside, 3rd edition, W.B. Saunders Company, Philadelphia, PA, USA, 2000.

19. Salle L, Kharche S, Zhang H, Brette F. Mechanisms underlying adaptation of action potential duration by pacing rate in rat myocytes. Progr Biophys Mol Biol 2008;96:305-20.

20. Sanguinetti MC, Tristani-Firouzi M. hERG potassium channels and cardiac arrhythmia. Nature2006;440:463-9